Selective binding of proteins on functional nanoparticles in a binary protein solution

Goutam Ghosh[1]*, Lata Panicker[2], Thomas J.Webster[3,4]
[1]UGC-DAE Consortium for Scientific Research, Mumbai Centre, Mumbai 400094, (INDIA)
[2]Solid State Physics Division, Bhabha Atomic Research Centre, Mumbai 400094, (INDIA)
[3]Department of Chemical Engineering, Northeastern University, Boston, MA 02115, (USA)
[4]Center of Excellence for Advanced Materials Research, King Abdulaziz University, Jeddah, (SAUDI ARABIA)
E-mail: ghoshg@csr.res.in; ghoshg@yahoo.com

ABSTRACT

The "reverse charge parity" model proposed by us establishes the selective electrostatic binding of charged proteins with oppositely charged functional iron oxide nanoparticles (IONP) in an aqueous solution [Ghosh *et al* 2014 *Mater. Res. Express* 1 015017]. In this paper, we have investigated the selectivity in binding of charged proteins with oppositely charged functional IONP in a binary protein solution. IONP was surface functionalized both positively (e.g., coated with cetylpyridinium iodide, or CPI) as well as negatively (e.g., coated with tri-lithium citrate, or TLC). The binary protein solution was prepared by mixing a 1:1 weight ratio of hen egg white lysozyme (HEWL) and ovalbumin (OVA) in water. HEWL (pI 11) is positively charged and OVA (pI 4.5) is negatively charged in water. The binding of proteins with functional IONP was characterized using several techniques, like, circular dichroism (CD), ultraviolet-visible (UV-vis), and fluorescence spectroscopy, ζ-potential and DLS. The results confirm the application of "reverse charge parity" model for selective binding of proteins with functional nanoparticles even in a mixed protein environment. The effect of counterions (e.g., I^- and Li^+) on the protein conformation has also been discussed briefly.   © 2015 Trade Science Inc. - INDIA

INTRODUCTION

Protein-nanoparticle interactions have been an important research area in view of the numerous applications of nanoparticles in medicine, especially, in diagnostics and therapeutics. The small size, functionalized surface, improved solubility, and multi-functionality of nanoparticles will continue to open many doors and create numerous possibilities in medical applications, such as targeted drug delivery[1–3], contrast enhancing agents for magnetic resonance imaging[4,5], hyperthermia treatment of cancer[6,7], etc. In particular, considerable research is being directed towards developing biodegradable polymers and polymeric (or polymer coated) nanoparticles for drug delivery and tissue engineering[8]. However, several difficulties arise when using

Full Paper

nanoparticles for in vivo applications preclinically and clinically[9], among which are biocompatibility, kinetics, tumor targeting efficiency, acute and chronic toxicity, ability to escape the reticuloendothelial system (RES), and cost-effectiveness[10]. All of these difficulties rely on initial protein interactions since it is proteins from the body which will adsorb within milliseconds, well before any cellular interactions take place. Moreover, the selectivity in binding of functional nanoparticles with proteins or any component of a living organism has been one of the main focus areas in nanoparticle research to circumvent such difficulties. However, few computational or mathematical models, like, antibody-receptor binding[11–13], hydrophobic binding[14–16], etc. have been used, so far, for the targeted binding of functional nanoparticles to proteins. The application of these models needs specific knowledge about nanoparticle targeting of proteins, cells, etc. inside the body. On the other hand, a general model, like electrostatic binding, needs no such prior knowledge. Selective binding of functional nanoparticles to a targeted substrate (like proteins or cells) using electrostatic attraction has not been explored elaborately, so far, except for a few publications[17,18].

The solid core of nanoparticles contributes very little to interactions with proteins, while surface ligands yield functional groups with apparent competence for long-range electrostatic and short-range hydrophobic or hydrogen bonding interactions[17]. Such ligand-coated gold nanoparticles have been studied in the context of biosensors[19], diagnostics[20], bionanomaterials[21], etc. In our recent papers[22–24], it was shown that charged functional iron oxide nanoparticles (IONP) selectively bind oppositely charged proteins due to the electrostatic interactions. We have also shown that the presence of counterions (e.g., Li$^+$ of TLC-IONP) irreversibly modifies secondary conformations of bound proteins. This effect was not seen in the absence of counterions (in 'aged' ligand-IONP dispersions) wherein the bound protein retained their native conformations. Accordingly, we propose a "reverse charge parity" model for the selective binding and denaturation of proteins by virtue of the protein-nanoparticle electrostatic interactions, and the model has been examined for various proteins[23].

It is important to note that the long-range interac-

tions control the proximity between proteins and nanoparticles, while the short-rang hydrophobic interactions are evident when the hydrophobic group on the functional nanoparticles (or the electrolytes) can access a hydrophobic domain on the protein[25]. On the other hand, the long-range electrostatic interaction is not limited in this way. When the net charge of proteins is of same sign as that on the functional nanoparticles, all short-range attractive forces must be balanced by long-range electrostatic repulsion[17,23]. However, when protein charge is opposite to that of the functional nanoparticles, electrostatic attraction will cause proteins to bind with nanoparticles. This binding is an indication of a protein "charge patch"[26–28]. Such surface charge anisotropy is protein specific[29].

Circular dichroism (CD) is an excellent and sensitive technique for rapidly evaluating the secondary structure, folding and binding properties of proteins[30,31], and their structural changes due to interactions with nanoparticles[22]. However, it does not give any residue-specific information[31].

In this work, we have investigated the application of "reverse charge parity" model for "selective" binding of charged proteins with oppositely charged functional IONP in a binary protein solution of hen egg white lysozyme, HEWL (pI~11), and ovalbumin, OVA (pI~4.5). IONP was surface functionalized both positively (e.g., coated with cetylpyridinium iodide, or CPI) as well as negatively (e.g., coated with tri-lithium citrate, or TLC). We have used several techniques to characterize protein bind, e.g., CD, UV-visible and fluorescence spectroscopy, ζ-potential and DLS techniques. The present investigation is expected to add useful knowledge towards *in vivo* physiological applications of charged functional nanoparticles.

MATERIALS AND METHODS

Materials

FeCl$_3$, 6H$_2$O (98%) was purchased from Burgoyne Burbidges & Co (India) and FeCl$_2$ (anhydrous; 99.5%), from Alfa Aesar (USA). NH$_4$OH (30% conc.) was purchased from Merck (India). Cetylpyridinium iodide (CPI, M.W. = 431.44 g.mol^{-1}, 98%), was purchased from Sigma-Aldrich (India) and tri-lithium citrate (TLC, M.W. = 281.99g.mol^{-1}, 98.5%), from S.D. Fine Chem.

Ltd., Mumbai, India. Hen egg white lysozyme, HEWL ($<M_w>$ = 14,300 g.mol^{-1}, L-6876) and ovalbumin, OVA ($<M_w>$ = 44,600 g.mol^{-1}, A-5503) were purchased from Sigma. All chemicals were used without any further purification. The milli-Q water was first obtained from a three-stage purification system (Millipore, USA) and then filtered again through a 0.22 μm filter and then autoclaved. The pH and the electrical resistivity of this water were found to be 6.5 and 18.2 MΩ cm$^{"1}$, respectively. This water was used for all sample preparation and measurements here.

Preparation of functional IONP dispersion

Iron oxide nanoparticles (IONP) were synthesized by a chemical co-precipitation reaction between Fe^{3+} and Fe^{2+} salts (Fe^{3+}:Fe^{2+} = 3:2) in basic aqueous medium[32]. Details of the synthesis procedure may be seen in one of our earlier papers[24]. The black precipitate was separated out using a strong permanent magnet underneath and the supernatant was discarded. The precipitate was washed several times using milli-Q water until the supernatant became neutral. Finally, the precipitate was washed with acetone and was left at room temperature for drying. The stoichiometry of the nanoparticles synthesized through this protocol has been reported to be Fe$_3$O$_4$[22]. The nanoparticle surface was functionalized (i.e., coated) with CPI and TLC following procedures reported earlier[22] and has been named as CPI-IONP and TLC-IONP here, respectively. They were dispersed in water at a concentration of 2.0 wt%.

Preparation of binary protein solution and its incubation with functional IONP

A 0.1 wt% stock solution of a binary mixture of HEWL and OVA at a weight ratio of 1:1 was prepared in water. There was no change in solution pH after the mixing of proteins. Aqueous dispersions of CPI-IONP and TLC-IONP, each at a concentration of 0.1 wt%, were prepared from the initial (i.e., 2.0 wt%) dispersions. The protein solution was further diluted (see below) to match the scale for CD measurements. Proteins and ligand-IONP were mixed at variable weight ratios of 1:x (for x = 0.5, 1.0, 1.5, and 2.0), as described below:

(i)   100 μl 0.1 wt% protein solution + 200 μl H$_2$O
(ii) 100 μl 0.1 wt% protein solution + v μl 0.1 wt%

ligand-IONP + (200 − v) μl H$_2$O

where v = 50, 100, 150 and 200. These dispersions were left on a shaker at 4°C for 48 h[22–24]. The interaction of two proteins (e.g., Protein1 and Protein2) with functional IONP (i.e., ligand-IONP) in the binary solution can be described by the following relationships:

(a)   Protein1 + Protein2 + ligand-IONP '! Protein1 (interacted) + Protein2 (uninteracted) + Protein1-ligand-IONP
      and,

(b)   Protein1 + Protein2 + ligand-IONP '! Protein1 (uninteracted) + Protein2 (interacted) + Protein2-ligand-IONP

'Protein1' and 'Protein2' on the left hand side of these relationships are in their native state. Proteins with 'interacted' and 'uninteracted' within brackets indicate those specific proteins which have interacted and have not interacted with ligand-IONP, respectively. 'Protein-ligand-IONP' corresponds to the conjugates of protein and ligand-IONP. In the above relations, we have assumed that 'Protein1' and 'Protein2' do not interact with each other. The 'Protein-ligand-IONP' conjugates eventually agglomerate and precipitate. Precipitates were separated out using the magnet and the supernatants have been used for the investigation of binding of selective proteins with ligand-IONP, as the concentration of proteins in the supernatant is less than that of the un-incubated binary solution. The above relationships indicate that 'ligand-IONP' conjugates develop a dynamic 'corona' of proteins whose number varies over time due to continuous association and dissociation in equilibrium.

Methods

The particle size (i.e., hydrodynamic diameter, D$_h$) and the ζ-potential of the ligand-IONP in dispersion before and after incubation with the binary protein solution [see relationships (a) and (b)] were measured using the Zetasizer Nano ZS (Malvern, UK) instrument. Ultra-violet (UV) absorption spectra of the binary protein solution, before and after incubation with ligand-IONP, were measured in the wavelength range of 190–400 nm using a Shimadzu (model: UV-1800, Japan) UV–visible spectrometer. Fluorescence absorption
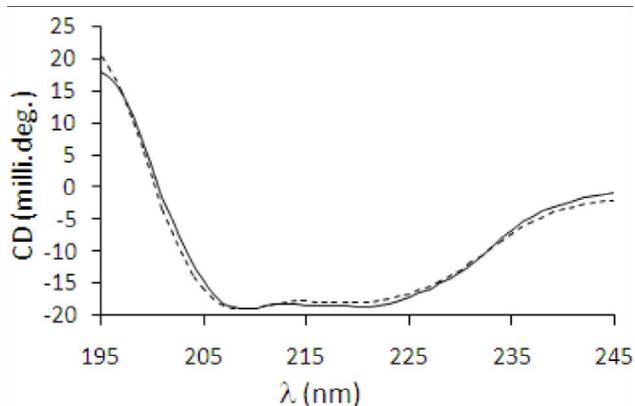
Full Paper

Figure 1: CD spectrum of the binary solution of HEWL and OVA, mixed at the weight ratio of 1:1 (—) and CD spectrum (—) generated by averaging the sum of the CD spectra obtained from HEWL and OVA solutions (see text for details)

spectra were measured in the wavelength range of 250 to 450 nm using a JASCO (model: FP-8500, Japan) fluorescence spectrophotometer. The excitation wavelength (λ_{ex}) used was 280 nm. CD spectra were measured using a JASCO (model: J-815, Japan) instrument in the wavelength range of 195–260 nm, and three runs per sample were taken for better statistics. All measurements were carried out at 25 ºC.

RESULTS

Circular dichroism spectroscopy

Far ultraviolet circular dichroism (CD) spectroscopy was used for characterizing the secondary conformations of proteins in a single (unitary) protein solution. In the CD spectrum of a protein, ±-helical conformations have negative bands at 222 and 208 nm and a positive band at 193 nm[33]. Proteins with well-defined anti-parallel ²-pleated sheets have a negative band at 218 nm and positive band at 195 nm[34], while disordered proteins have very low ellipticity above 210 nm and negative bands near 195 nm[35]. Deconvolution of the CD spectrum gives relative contents of different secondary conformations of the protein. In the present investigation, we have used the CD technique to characterize the binary protein solution of HEWL and OVA before and after incubation (i.e., interaction) with the charged ligand-IONP. HEWL and OVA are known to be ± and ² proteins, respectively. Therefore, HEWL shows a stronger absorbance minimum at 208 nm and a weak broad (overlapping of two minima due to ±-
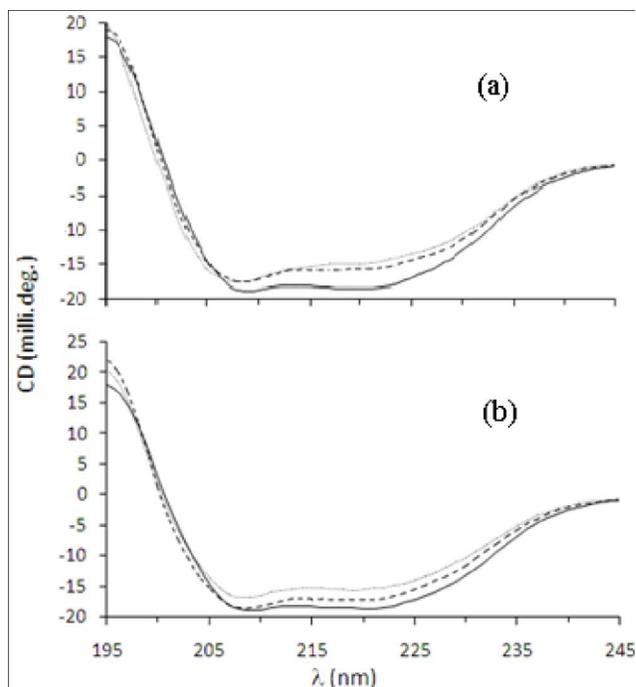

Figure 2: CD spectra of the binary solutions of HEWL and OVA before (—) and after incubation with (a) CPI-IONP; (b) TKC-IONP at weight ratios of 1:1 (—) and 1:2 ('''''''''').

helix and ²-sheet conformations) absorbance minimum between 218 and 222 nm[22]. On the other hand, OVA shows a strong broad absorbance minimum between 218 and 222 nm, with a weaker absorbance minimum at 208 nm[23]. Since the binary solution contains a mixture of two different proteins, deconvolution of the corresponding CD spectrum is difficult. Hence, we have reported the changes appeared in the CD spectra before and after incubation with charged ligand-IONP. The CD spectrum from the binary solution (solid line) before incubation with ligand-IONP is shown in Figure 1. The dashed line spectrum is generated by averaging the sum of the CD spectra obtained from HEWL and OVA solutions (for example, reference 23), both at a concentration of 0.033 wt%. A reasonably good agreement between the two spectra indicates that the interaction between HEWL and OVA was negligible and the secondary conformations of HEWL and OVA in the binary solution were similar to that observed in the individual protein solution. We have calculated the ratio, $R_{\Delta A}$, of the intensities of minima at 208 nm (i.e., ΔA_{208}) and at 222 nm (i.e., ΔA_{222}) for HEWL and OVA solutions and their binary solution, and the values are 1.31, 0.85 and 1.07, respectively.

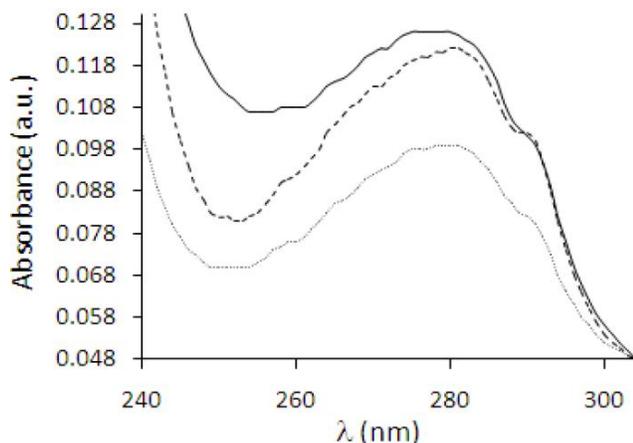Figure 2 shows the CD spectra of the binary so-

Goutam Ghosh et al.

Full Paper

Figure 3: UV absorption spectra of the binary solutions of HEWL and OVA before (—) and after incubation with CPI-IONP (—) and TKC-IONP ('''''''') at a weight ratio of 1:2

Figure 4: Fluorescence emission spectra of the binary solutions of HEWL and OVA before (—) and after incubation with CPI-IONP (—) and TKC-IONP ('''''''), at a weight ratio of 1:2. The excitation wavelength, λ_{ex} = 280 nm.

lutions before (—) and after incubation with (a) CPI-IONP and (b) TLC-IONP at the weight ratios of 1:1 (—) and 1:2 ('''''''). From Figure 2(a) we observe that after incubation the intensity of the minimum between 218 and 222 nm decreased more significantly than that at 208 nm and the $R_{\Delta A}$ was measured to be 1.12 and 1.20, respectively, for the 1:1 and 1:2 spectra. The small change in $R_{\Delta A}$ may be confused with experimental error. Therefore, we measured this ratio from several CD spectra and confirmed the trend of $R_{\Delta A}$ with the CPI-IONP concentration in the binary solution. This trend indicates that the OVA bound with the positively charged CPI-IONP. Similarly in Figure 2(b), $R_{\Delta A}$ decreases with increasing concentration of TLC-IONP, indicating the binding of HEWL with TLC-IONP.

UV-visible spectroscopy

Figure 3 shows the ultraviolet (UV) absorption band at 280 nm for the binary solutions of HEWL and OVA before (—) and after incubation with CPI-IONP (—) and TLC-IONP ('''''''') at a weight ratio of 1:2. The UV band intensity was seen to decrease from the un-incubated solution towards the solutions incubated with CPI-IONP and TLC-IONP, respectively. This result indicates that more number of HEWL, compared to OVA, binds with the oppositely charged ligand-IONP in the binary solution. This is in agreement with the CD results.

Fluorescence spectroscopy

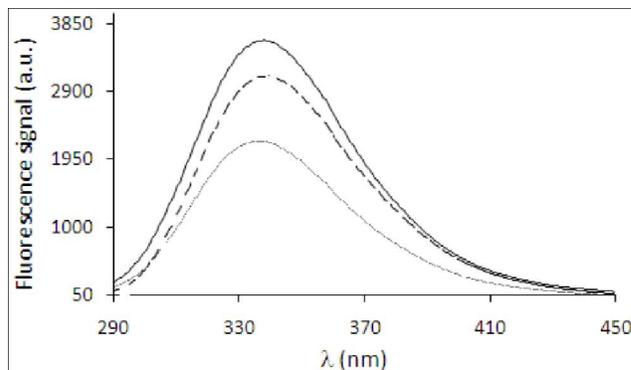Fluorescence quenching is frequently employed to study interactions with proteins. Any process which

decreases the fluorescence emission intensity of a sample is termed quenching. The quenching occurs through either static or dynamic mechanism. In static mechanism, when a protein binds with substrate forms a non-fluorescence complex. As a result, the fluorescence band quenches. In the present investigation, the binding of proteins with ligand-IONP has been investigated through the fluorescence quenching experiment. Figure 4 shows the fluorescence emission bands at around 340 nm from the binary protein solutions of HEWL and OVA (1:1)before (—) and after incubation with CPI-IONP (—) and TLC-IONP ('''''''') at a weight ratio of protein:ligand-IONP = 1:2. The quenching of the fluorescence band of protein after incubation of the binary with ligand-IONP indicates formation of 'protein-ligand-IONP' non-fluorescence complexes. The binding of protein with ligand-IONP must be due to electrostatic attraction and a stronger attraction was observed with TLC-IONP than CPI-IONP.

ζ-potential and DLS measurements

The ζ-potential and DLS measurements of the ligand-IONP conjugates were carried out before and after incubation with the binary protein solution. Figure 5 shows the ζ-potential distributions corresponding to the: (a) TLC-IONP solution, (b) CPI-IONP solution, (c) binary solution of HEWL and OVA (at 1:1), (d) the binary solution after incubation with CPI-IONP (at 1:2), and (e) the binary solution after incubation with TLC-IONP (at 1:2). Figure 5(c) shows the double distribution at around -8.0 mV and +1.0 mV corresponding to OVA and HEWL, respectively. Figure 5(d) shows the absence of OVA indicating the "selective" binding
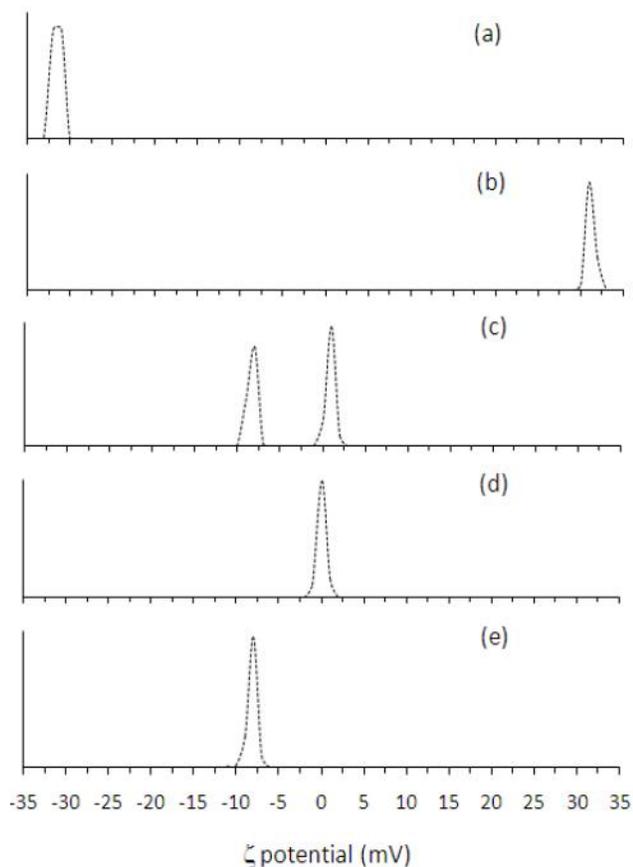
Full Paper

Figure 5: ζ-potential distributions of the dispersions of (a) TLC-IONP, (b) CPI-IONP, (c) mixture of HEWL and OVA at a 1:1 weight ratio, (d) HEWL and OVA after incubation with CPI-IONP, and (e) HEWL and OVA after incubation with TLC-IONP.

of OVA with CPI-IONP in the binary solution. Similarly from Figure 5(e), we can infer that HEWL selectively bound with TLC-IONP in the binary solution. This result again proved the validity of the "reverse charge parity" model in a binary solution. The protein binding with the oppositely charged ligand-IONP is also confirmed by measuring the size (i.e., hydrodynamic diameter) of CPI-IONP and TLC-IONP conjugates in the corresponding dispersions, using the DLS technique, before and after incubation with the binary protein solution (figure not shown). The size of both CPI-IONP and TLC-IONP conjugates was measured to be around 40 nm before incubation with the binary solution. After incubation the size was observed to be around 500 nm, indicating aggregation due to surface charge neutralization after binding of charged proteins with charged ligand-IONP supporting the "reverse charge parity" model.
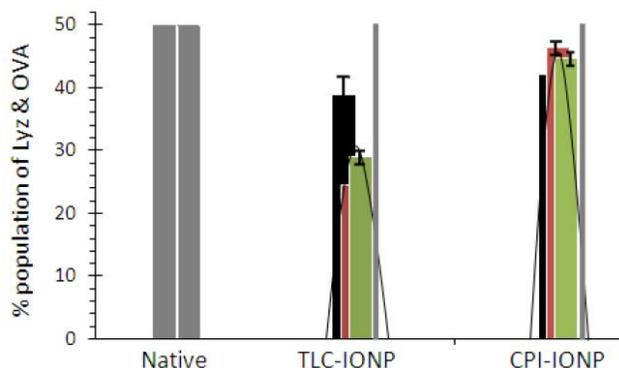

Figure 6: Bar diagrams of calculated amounts of HEWL and OVA in the binary solutions, before ('native') and after incubation with TLC-IONP and CPI-IONP, at a weight ratio of 1:2. The bars with *brown*, *green* and *black* colors represent the values obtained from fluorescence, UV and CD spectra, respectively. The *grey* narrow bars at 'TLC-IONP' and 'CPI-IONP' represent 100% presence of OVA and HEWL, respectively, in the binary solution after incubation with the corresponding ligand-IONP

DISCUSSION

The percentage of protein binding (i.e., either HEWL or OVA) with the oppositely charged ligand-IONP in the binary solution was qualitatively calculated from the decrease in integrated intensities of CD, UV absorption and fluorescence emission spectra of binary solutions after incubation with ligand-IONP at a 1:2 weight ratio. The percentage binding of OVA and HEWL were calculated to be approximately 16.0 ± 2.0 and 22 ± 4.0, respectively, from CD spectra. Similarly, from UV absorption and fluorescence emission spectra the percentage binding of OVA and HEWL with CPI-IONP and TLC-IONP was calculated to be 7.0 ± 2.0 and 50.8 ± 5.0, and 9.6 ± 2.0 and 42 ± 1.0, respectively. More binding of HEWL with ligand-IONP may correspond to the fact that HEWL is a smaller protein, and therefore, diffuses faster than OVA in the binary solution; eventually causing more binding with the ligand-IONP. In Figure 6, we have shown the bar diagram to represent the percentage contents (100 " calculated % binding) of HEWL and OVA in the binary solution before ('native') and after incubation with TLC-IONP and CPI-IONP at a weight ratio of 1:2. The bars with *brown*, *green* and *black* colors represent the values obtained from fluorescence, UV and CD spectra, respectively. The *grey* narrow bars at 'TLC-IONP'
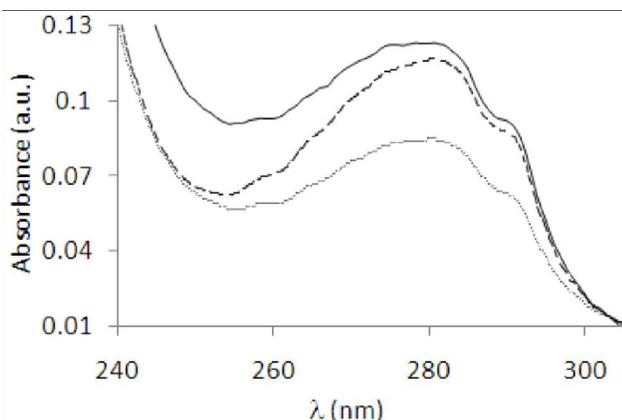
Figure 7: UV absorption spectra of the binary solutions A: (—), B: (—-) and C: ('""""""), see text for details.

Figure 8: CD spectra of the binary solution after incubation with (a) TLC-IONP (o) and (b) TKC-IONP ("), at a 1:1 weight ratio. The *red* spectrum in (a) is obtained by averaging the sum of the CD spectra of un-incubated OVA solution, and HEWL solution after incubation with TLC-IONP at a weight ratio of 1:1. The *green* spectrum in (b) is obtained by averaging the sum of the CD spectra of the un-incubated HEWL solution, and OVA solution after incubation with CPI-IONP at a 1:1 weight ratio

and 'CPI-IONP' represent unabsorbed 'native' OVA and HEWL, respectively, in the binary solution.

To verify above calculated values, we prepared three binary solutions of HEWL and OVA at three different weight ratios corresponding to the mean percentage contents of proteins, as represented in Figure 6, as described below,

A   100 µl 0.1 wt% protein solution (HEWL:OVA = 1:1) + 200 µl H_2O

B   100 µl 0.1 wt% protein solution (HEWL:OVA = 1:0.89) + 200 µl H_2O

C   100 µl 0.1 wt% protein solution (HEWL:OVA = 0.62:1) + 200 µl H_2O

Where A, B and C represent the binary solutions before (un-incubated) and after incubation with CPI-IONP and TLC-IONP, respectively. We have measured the UV absorption spectra of these solutions which are shown in Figure 7. Solid, dashed and dotted curves represent the solutions A,

B and C, respectively. These spectra match well with the UV absorption spectra of binary solutions taken before and after incubation with ligand-IONP (Figure 3). This result reveals that our binding calculation based on the "reverse charge parity" model was more or less correct. Therefore, we can infer here that the "reverse charge parity" model can be used for "selective" binding of charged proteins with oppositely charged functional nanoparticles in any mixed protein solution like the physiological environment.

As described earlier, the $R_{\Delta A}$ indicates that HEWL or OVA selectively binds with the oppositely charged ligand-IONP in the binary protein solution. This has been demonstrated by Figure 8. Figure 8(a) shows the CD
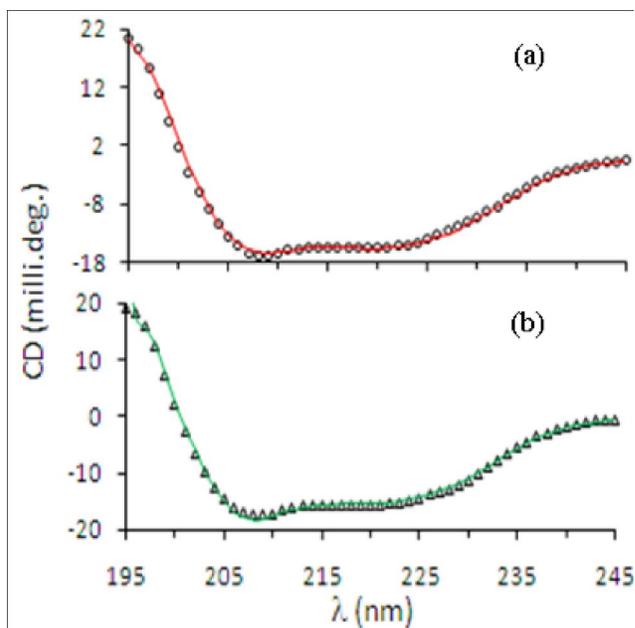
spectrum (o) of the binary solution after incubation with TLC-IONP at a 1:1 weight ratio. The red spectrum was obtained by averaging the sum of the CD spectra of the un-incubated OVA solution[23], and HEWL solution after incubation with TLC-IONP at the weight ratio of 1:1 [24]. A good agreement between the two CD spectra clearly suggests that the positively charged HEWL binds with the negatively charged TLC-IONP in the binary solution. Similarly, Figure 8(b) shows the CD spectrum (Δ) of the binary solution after incubation with CPI-IONP (Δ) at a 1:1 weight ratio. The green spectrum was obtained by averaging the sum of the CD spectra of the un-incubated HEWL solution, and OVA solution after incubation with CPI-IONP at a 1:1 weight ratio. Again, a good agreement between the two indicates the binding of the negatively charged OVA with the positively charged CPI-IONP in the binary solution. This result again proves the validity of the "reverse charge parity" model in the binary protein solution. Figure 8 also reveals the fact that the effect of counterions, namely, Li^+ and I^-, on the secondary struc-

Full Paper

ture of proteins in the binary protein solution was similar to that reported previously in unitary solutions[23,24]. Though the interaction between proteins and ligand-IONP will usually be less in a binary solution than in a unitary solution due to the effect of screening, nevertheless, the "reverse charge parity" model is seen to be valid in the binary protein solution.

CONCLUSIONS

In this paper, we have investigated the application of the "reverse charge parity" model in a binary protein solution. The binding of proteins with functional IONP has been characterized by different spectroscopy techniques, as well as by ζ-potential and particle size measurement techniques. Our results showed that charged proteins in the binary solution "selectively" bind with the oppositely charged functional IONP establishing the validity of the "reverse charge parity" model in selective protein-nanoparticle binding applications. A smaller protein (e.g., HEWL) binds more than a larger protein (e.g., OVA), in the binary solution, due to more diffusion coefficient. The effect of counterions on the secondary structure of the 'selectively' bound protein was same as observed in a unitary protein/ligand-IONP solution. Though the physiological environment is more compound than a binary protein solution, still a simple model of selective binding of proteins with functional nanoparticles for medical applications could be established through this investigation which is novel.

REFERENCES

[1] R.Singh, J.W.Lillard; Jr. Exp. Mol. Pathol., **86**, 215 **(2009)**.

[2] V.V.Mody, A.Cox, S.Shah, A.Singh, W.Bevins, H.Parihar; Appl. Nanosci., **4**, 385 **(2014)**.

[3] S.A.Mackowiak, A.Schmidt, V.Weiss, C.Argyo, C.von Schirnding, T.Bein, C.Bräuchle; NanoLett,. **13**, 2576 **(2013)**.

[4] J.Huang, L.Wang, R.Lin, A.Y.Wang, L.Yang, M.Kuang, W.Qian, H.Mao; ACS Appl. Mater. Interfaces, **5**, 4632 **(2013)**.

[5] S.H.Lee, H.B.Na, T.Hyeon; Wiley Interdiscip. Rev. Nanomed. Nanotechnol, **6**, 196 **(2014)**.

[6] J.Zee.van der; Ann. Oncol., **13**, 1173 **(2002)**.

[7] M.H.Falk, R.D.Issels; Int. J. Hyperthermia, **17**, 1

[8] J.Kreuter; 1994 in Encyclopaedia of Pharmaceutical Technology; New York:Marcel Dekker Inc. 165 **(1994)**.

[9] W.Cai, T.Gao, H.Hong, J.Sun; Nanotechnology, Science and Applications, **1**, 17 **(2008)**.

[10] W.Cai, X.Chen; Small, 1840, **3 (2007)**.

[11] M.Rothdiener, J.Beuttler, S.K.E.Messerschmidt, R.E.Kontermann; Methods Mol. Bio., **624**, 295 **(2013)**.

[12] L.Yang, H.Mao, Y.A.Wang, Z.Cao, X.Peng, X.Wang, C.Ni.H.Duan, Q.Yuan, G.Adams, M.Q.Smith, W.C.Wood, X.Gao, S.Nie; Small, **5**, 235 **(2009)**.

[13] S.C.Owen, N.Patel, J.Logie, G.Pan, H.Persson, J.Moffat, S.S.Sidhu, M.S.Shoichet; J. Controll. Release, **172**, 395 **(2013)**.

[14] J.Klein; Proc. Nat. Acad. Sci., USA , **104**, 2029 **(2007)**.

[15] I.Lynch, K.A.Dawson; Nanotoday , **3**, 40 **(2008)**.

[16] R.A.Sperling, W.J.Parak; Phil. Trans. R. Soc., **A368**, 1333 **(2010)**.

[17] K.Chen, Y.Xu, S.Rana, O.R.Miranda, P.L.Dubin, V.M.Rotello, L.Sun, X.Guo; Biomacromolecules, **12**, 2552 **(2010)**.

[18] R.Khandelia, J.Deka, A.Paul, A.Chattopadhyay; RSC Advances, **2**, 5617 **(2012)**.

[19] C.C.You, O.R.Miranda, B.Gider, P.S.Ghosh, I.B.Kim, B.Erdogan, S.A.Krovi, U.Bunz, V.M.Rotello; Nat. Nanotechnol, **2**, 318 **(2017)**.

[20] R.L.Phillips, O.R.Miranda, C.C.You, V.M.Rotello, U.Bunz U ; Angew. Chem., Int. Edition, **47**, 2590 **(2008)**.

[21] R.A.Mcmillan, C.D.Paavola, J.Howard, S.L.Chan, N.J.Zaluzec, J.D.Trent; Nat. Mater, **1**, 247 **(2002)**.

[22] G.Ghosh, L.Panicker, R.S.Ningthoujam, K.C.Barick, R.Tewari; Colloid. Surf., **B103**, 267 **(2013)**.

[23] G.Ghosh, L.Panicker, K.C.Barick; Mater. Res. Express, **1**, 015017 **(2014)**.

[24] G.Ghosh, L.Panicker, K.C.Barick; Colloid. Surf., B **118,** 1 **(2014)**.

[25] J.Y.Gao, P.L.Dubin; Biopolymers, **49**, 185 **(1999)**.

[26] E.Seyrek, P.L.Dubin, C.Tribet, E.A.Gamble; Biomacromolecules , **4**, 273 **(2003)**.

[27] C.G.de Kruif, F.Weinbreck, R.de Vries; Curr. Opin. Colloid Interface Sci., **9**, 340 **(2009)**.

[28] R.de Vries; J. Chem. Phys., **120**, 3475 **(2004)**.

[29] Y.Nozaki, L.G.Bunville, C.Tanford; J. Am. Chem. Soc., **81**, 5523 **(1995)**.

[30] G.D.Fasman; Circular Dichroism and the Conformational Analysis of Biomolecules; New York: Ple-

num Press **(1996)**.

[31] N.J.Greenfield; Nat. Protoc.*,* **1**, 2876 **(2006)**.

[32] L.P.Ramirez, K.Landfester; Macromol. Chem. Phys., **204**, 22 **(2003)**.

[33] G.Holzwarth, P.Doty; J. Am. Chem. Soc., **87**, 218 **(1965)**.

[34] N.Greenfield, G.D.Fasman; Biochemistry, **8**, 4108 **(1969)**.

[35] S.Venyaminov, I.A.Baikalov, Z.M.Shen, C.S.Wu, T.J.Yang; Anal. Biochem., **214**, 17 **(1993)**.